

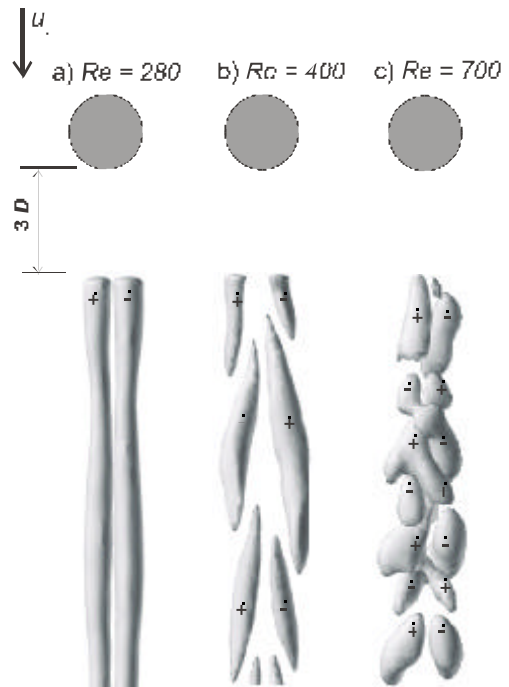
Spatio-temporal reconstruction of the unsteady wake of axi-symmetric bluff bodies via time-recording DPIV

by

Christoph Brücker

Aerodynamisches Institut der RWTH Aachen
Wüllnerstr. Zw. 5 u. 7,
D-52062 Aachen, Germany
E-mail: bruecker@aia.rwth-aachen.de

Abstract. The present study was undertaken with the objective of a more detailed quantitative analysis of the evolution of the flow field in the wake of axisymmetric bluff bodies like spheroids or bubbles. With the measurement technique described here, we could confirm that the form of the flow field predicted by Schwarz et al. also arises for a solid sphere which is a more close approximation to the shape of a bubble. The figure below shows the spatio-temporal reconstruction of the streamwise vorticity in the wake of a sphere for three different Reynolds-numbers. The sphere was placed in the test section of the water tank and the secondary flow in the wake was measured in a horizontal plane three diameters downstream of the sphere. The flow field and streamwise vorticity distribution in the plane was obtained by chronological DPIV recordings. A three-dimensional data cube was created from the temporal evolution of the planar vorticity distribution by stacking the results of continuous successive moments in the vertical direction. The spatio-temporal reconstruction of the vortex structures is displayed by means of surfaces of constant streamwise vorticity within the three-dimensional data cube. For $Re = 280$ the wake is continuous and consists clearly of a pair of streamwise vortices. A slight waviness in the size and strength of the vortices can be seen. For $Re = 400$ hairpin-vortices are periodically shed in the wake. The reconstructed streamwise structures in the figure represent the legs of the hairpin vortices. Note that the measurement results demonstrate a chain of oppositely oriented hairpin-vortices with alternate circulation as also observed by Johnson & Patel. Finally, in the case when $Re = 700$ the wake structure allows us to recognize phases, in which – besides an irregular orientation of the hairpin-vortices - the shedding is partly suppressed and the structure is twisted as a whole into a double-helical vortex structure. Such a phase is shown at the right-hand side. One can see the beginning and end of this phase by means of the open legs at the top and bottom end of the structure, which mark the generation of the shed hairpin with opposite circulation.



INTRODUCTION

The present study was undertaken with the objective of a more detailed quantitative analysis of the evolution of the flow field in the wake of axi-symmetric bluff bodies like spheroids or bubbles. Much data exist for the wake of nominally two-dimensional bodies like the wake of a cylinder. On the other hand, the wake of axi-symmetric bodies exhibits grave differences in the shape and dynamic of the vortices being shed in comparison to the two-dimensional case. The wake structures are basically three-dimensional and unsteady which makes the measurement and interpretation difficult. Up to now, experiments providing detailed instantaneous flow field data in the wake do not exist. Therefore, our current day knowledge about the vortical structures contained in the wake, is still based mainly on earlier flow visualization studies. A pair of attached vortices was observed by Nakamura¹ for sphere wakes in the range $210 < Re < 270$. For higher Reynolds-number up to $Re = 490$, the flow visualization experiments revealed a shedding of hairpin-like vortex structures²⁻⁴. The wake appears as a chain of hairpin-vortices with the heads pointing always to the same side. However, any flow pattern visualized with dye-injection technique always depend on the way how and where the dye is released into the flow. Recent numerical simulations of the sphere wake flow by Johnson and Patel demonstrated that most of the flow visualization results have overlooked vortex structures in the wake which are induced within the fluid and are not connected with the base of the bluff body⁵. These occur as oppositely oriented hairpin-vortices in between the one-sided chain of hairpin-vortices seen in the flow pictures from Nakamura etc. This further highlights that detailed chronological flow field measurements are necessary in order to provide the velocity and vorticity information for the entire bubble wake.

In our work, we investigate the structure and dynamics of the streamwise vortices in the wake by chronological high-speed PIV recordings which were captured in radial cross-sections downstream of the axi-symmetric bluff bodies. A digital high-speed camera records the flow and the DPIV results are analyzed by spatio-temporal reconstruction technique of the streamwise vorticity in the wake.

EXPERIMENTAL SET-UP

Our investigation focused on the spatial structure and dynamics of the streamwise vortices in the wake of axi-symmetric bodies. The flow field in the wake was recorded with a digital high-speed camera and evaluated frame-by-frame with the method of Digital-Particle-Image-Velocimetry (DPIV). As test-objects we used a solid sphere and a cylindrical rod with an elliptical nose and a sharp trailing edge, which was aligned with its axis along the flow axis (Fig. 1). In difference to the sphere, this cylinder has a defined separation edge and the boundary layer thickness is controlled by the length of the cylinder. This allows us to study the effect of the boundary layer thickness on the stability of the wake.

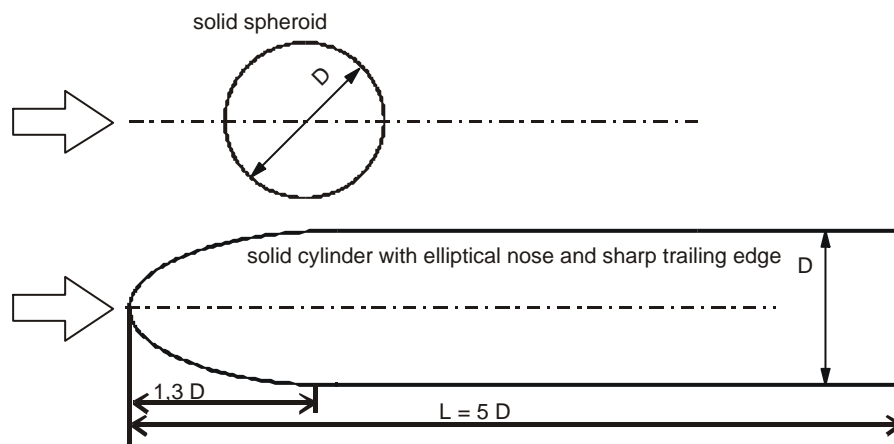


Fig. 1: Shape of the two axi-symmetric bluff bodies used in this study

The experiments were carried out in a vertical water channel shown in Fig. 2. The test section of transparent acrylic plates has a cross-section of 10×10 -cm square and is 1.2 m high. The bluff bodies with a diameter of 3 cm

were held in vertical position by a thin hollow tube of 2 mm diameter in the center of the channel. The boundary layer fluid along the tube in the part upstream of the fixation of the body is sucked through tiny holes into the tube to eliminate its effect on the flow around the body. Flow is driven by the constant head of the water in the settling chamber at the top of the channel and is controlled by a valve at the right-hand side bottom end of the test section. Upstream of the inlet into the test section, a contraction zone with a reduction rate by a factor of 5 is placed to provide a uniform flow with low turbulence level. Demineralized water was used as test liquid. Small tracer particles (Vestosint, mean diameter of $30\ \mu\text{m}$, $\rho = 1.02\ \text{g/cm}^3$) were added to the fluid upstream in the water basin and were mixed homogenous. The DPIV set-up was arranged to measure the velocity field in a horizontal cross-section, downstream of the body, (see the optical arrangement in Fig. 2), in order to obtain the streamwise component of the vorticity vector from the results. This is of importance for the understanding of the arrangement of the hairpin vortices and their legs which should leave a distinct pattern of the streamwise vorticity in the wake. The beam of a continuous Ar+ laser was expanded with a rotating polygonal mirror to form an intense virtual light-sheet in a horizontal cross-section of the channel. A digital high-speed video camera (Weinberger GmbH, Germany, resolution: 512×512 pixel; maximum frame rate: 1000 Hz, maximum number of frames: 2048) was used to record the flow, synchronized with the polygonal mirror so that each frame corresponds to a single sweep of the laser beam.

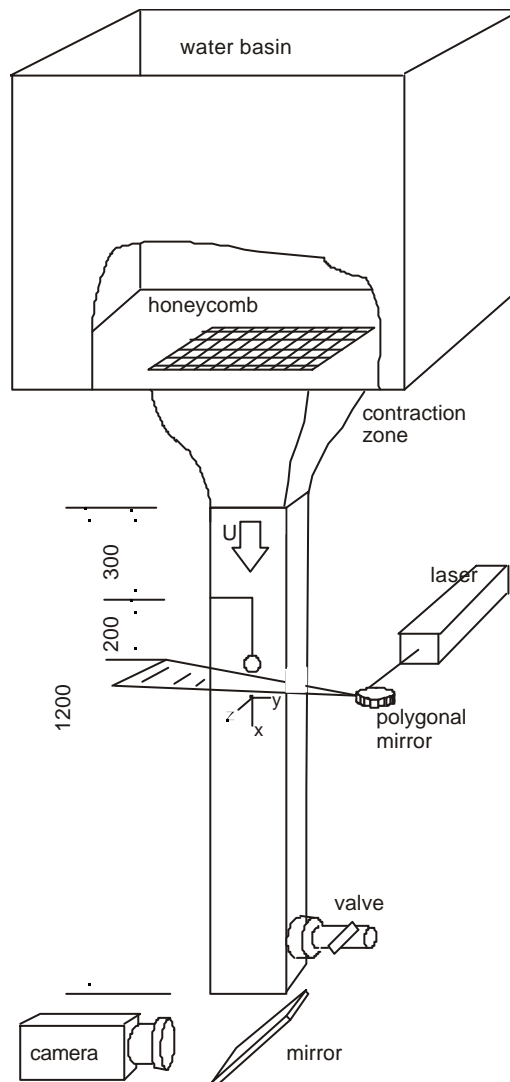


Fig. 2: Experimental set-up

Within the horizontal light-sheet plane (x - y plane), see the coordinate system in the channel as defined in Fig. 2, the in-plane velocity components were obtained from cross-correlation of successive images in small interrogation windows with a size of 32×32 pixel. The results represent a two-dimensional data set, in form of velocity vectors $\vec{u}(x, y)$ on a grid with 31×31 equidistant nodes over a squared cross-section area of $5 \times 5 \text{ cm}^2$, see Fig. 3. The streamwise vorticity component was determined out of the velocity field by calculating the gradients in the 3×3 neighbourhood of each node using central difference schemes.

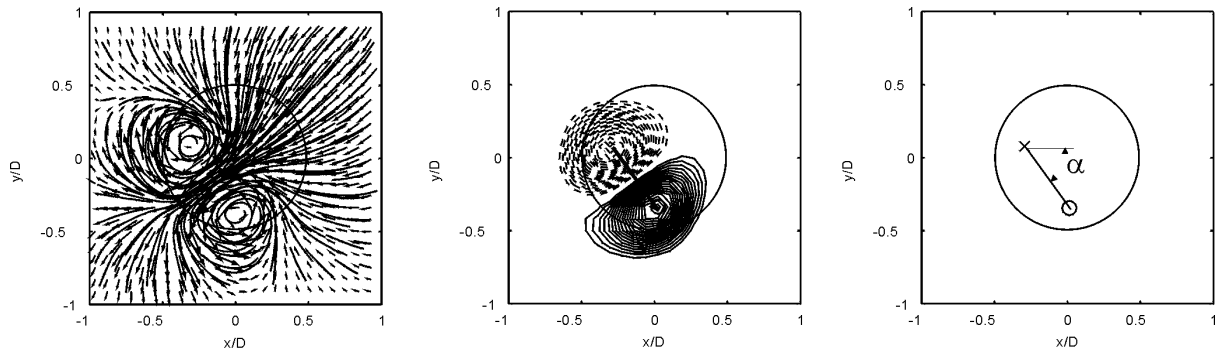


Fig. 3: Example of DPIV result in a horizontal plane in the wake of the sphere (left: velocity field and sectional streamlines; middle: vorticity field; right: angular orientation of the wake)

RESULTS

Before we discuss the results by means of the spatio-temporal reconstruction images, it is important to understand the reconstruction procedure. Therefore, the dynamic of the wake of the bluff bodies is first shown by a sequence of DPIV results, see Fig. 5, for which we explain the reconstruction in detail.

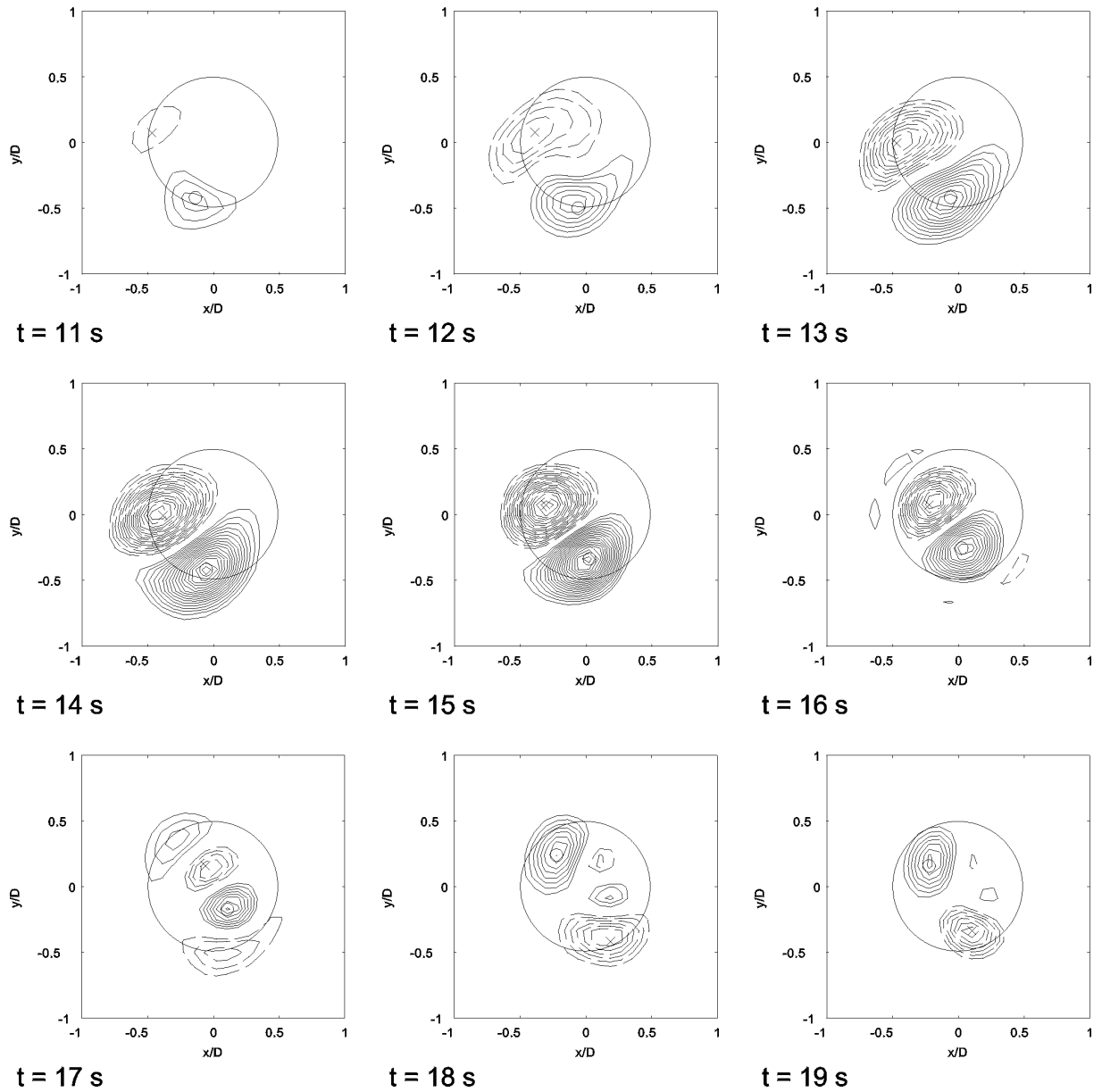
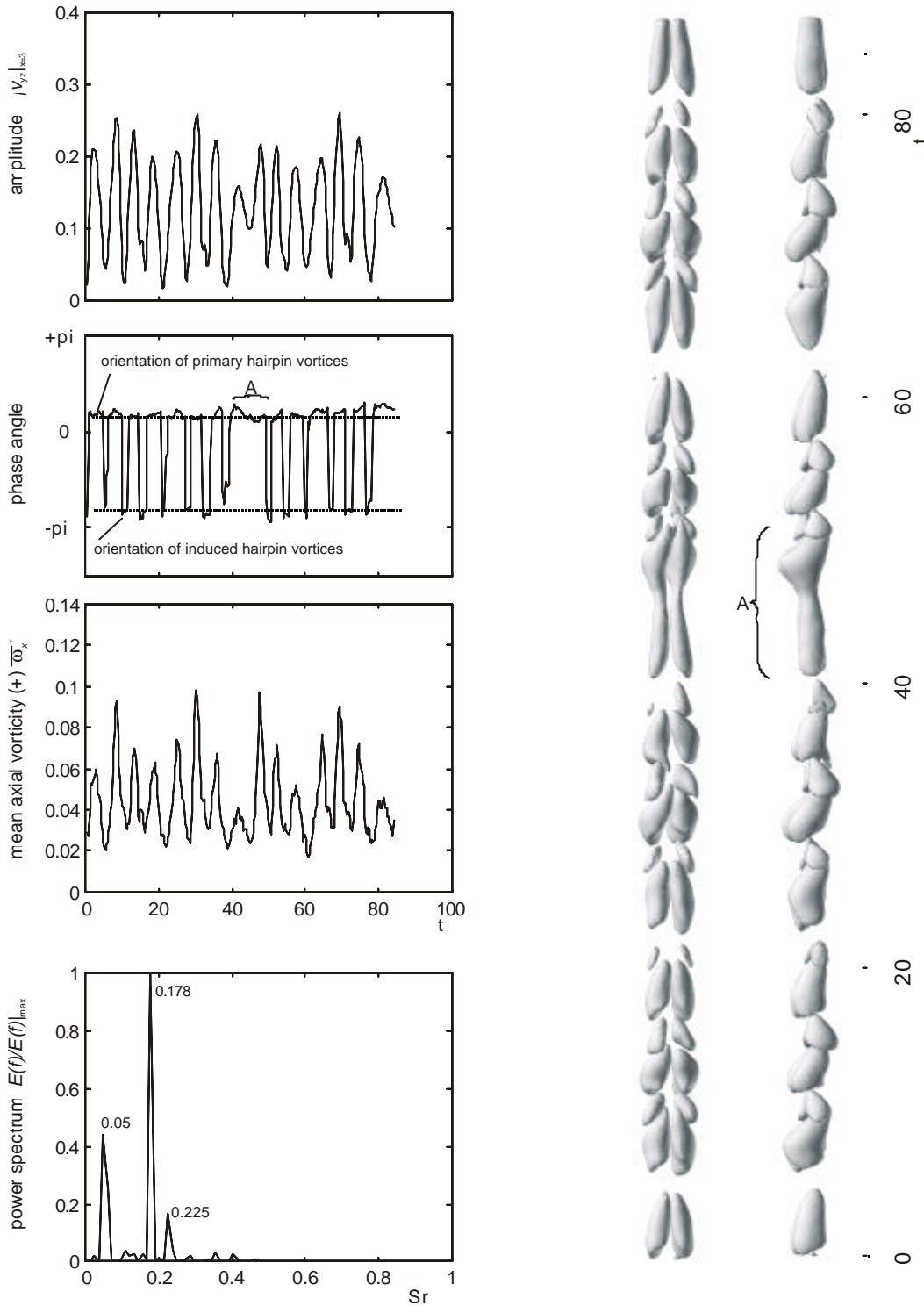


Fig. 4: Evolution of the streamwise vorticity distribution in a cross-section in the wake of a sphere ($Re = 500$)

From such a time sequence the spatio-temporal reconstruction of the vorticity field is created as follows. The vorticity values in the horizontal plane were taken, and stacked plane by plane vertically in a data cube over the complete sequence of DPIV results in the recorded period. The resulting data matrix can be displayed as an iso-



surface giving the spatio-temporal evolution of the component of streamwise vorticity at a stationary location within the wake. To reduce the high-frequency part and enhance the global pattern in the reconstruction image the surfaces were finally smoothed by a moving average technique. The following figure displays such a spatio-temporal reconstruction of the sphere wake for a Reynolds-number of $Re=500$, in addition to the graphical presentation of the temporal profiles of the amount and direction of the radial velocity component at the centerline as well as the variation of the amount of streamwise vorticity in the vortex cores.

HK500

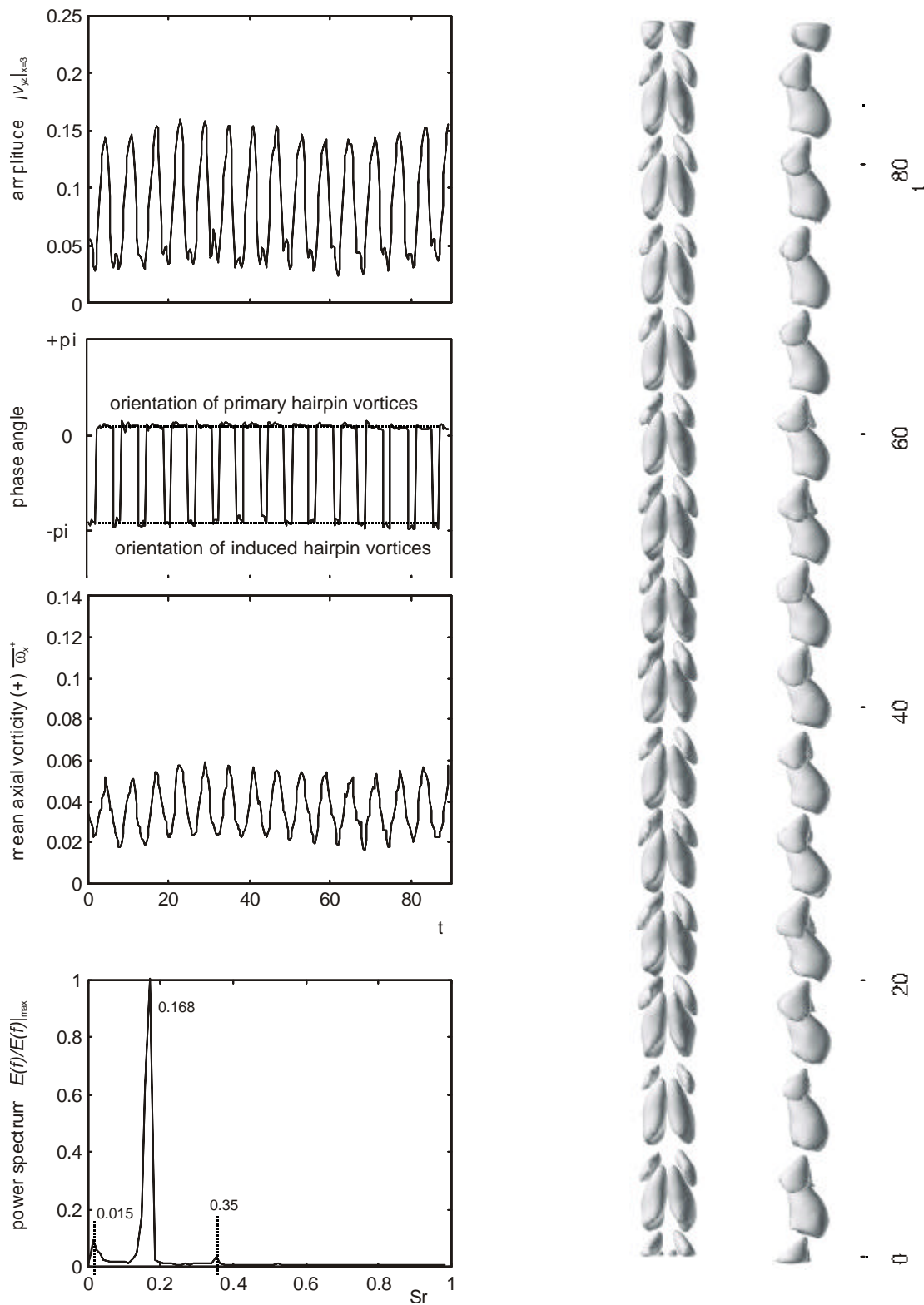


Fig. 6: Variation of amount and orientation of induced cross-flow in the sphere wake and spatio-temporal reconstruction of the streamwise vorticity distribution ($Re = 500$)

Fig. 7: Variation of amount and orientation of induced cross-flow in the cylinder wake and spatio-temporal reconstruction of the streamwise vorticity distribution($Re = 500$)

Both examples at the same Reynolds-number let clearly recognize the periodic shedding of alternately opposite oriented vortex pairs within nearly the same plane. Comparing our results with the figures published by Johnson & Patel one can see that the pairs represent parts of the actual three-dimensional hairpin-like vortices being shed in the wake, namely the streamwisely oriented parts of the legs. A remarkable feature of our results in agreement with the numerical results is the fact that the one-sided chain of vortex pairs is interconnected with counter-oriented vortex pairs of seemingly lower strength. A measure of the circulation of the hairpin-like vortices is the streamwise vorticity in the core of the legs which we calculated out of our data. Surprisingly, it turns out that the amount of streamwise vorticity in the legs does not reach the same maximum values in the “zig” and “zag” parts of the cycle. This obvious asymmetry (different amount of circulation) of the hairpin-vortices gives a strong indication that the bluff body experiences a net-lift force as found by Johnson & Patel⁵, too. In addition to a periodic fluctuating lift force, they observed a small offset of the average lift, indicating a stationary part of the lift force. The calculated vortical structure was found to show not only the typical sequence of shed hairpin-vortices but additional oppositely oriented induced hairpin-vortices, which do not have the same circulation as the shed ones. These previously unrevealed induced structures - as they describe - are generated by the interaction of the near wake flow and the outer flow and are based on a different mechanism as the shed hairpins. It is clearly demonstrated in Fig. 29 of their article, that the amount of streamwise vorticity of the shed hairpin-vortices is larger than that of the induced ones which agrees with our observation of different strength of the hairpin-vortices.

A comparison of the wake of the sphere with the cylinder shows that the boundary layer thickness has a strong influence on the stability and coherence of the flow. In comparison to the sphere, the wake of the axially oriented cylinder (with a larger thickness of the boundary layer) is approximately perfect periodic in time with a stable orientation of the vortices. Recognize the strong coherence of left-right alternation which demonstrates the near periodic creation and discharge of the vortices. The transition of the wake is overall shifted to higher Reynolds-numbers than that reported for the sphere wake flow, see e.g. Nakamura et al. An interesting feature can be deduced from the variation of the strength of the vortices over time. There is a slight low-frequency modulation of the overall strength of the vortices which appears as a small peak in the spectrum at $Sr = 0.015$ in addition to the peak at $Sr = 0.168$ representing the primary periodic shedding. This low-frequency modulation was also observed by Schwarz et al. in their numerical simulation. In comparison, the sphere wake exhibits slight random variations of the orientation of the vortices. Similar as in the case of the cylinder wake, there is a low-frequency modulation of the strength of the vortices which can be found in the spatio-temporal reconstruction image, too. The vortices seem to be shed in “pockets” of 3 to 4 hairpin-vortices, interrupted by phases with only low action. In one of these phases the shedding is completely suppressed which is marked as phase “A” in figure 6. This clearly shows, that there is an interaction of instabilities at different characteristic frequencies which was not observed in experiments before. Note that the peak of the low-frequency modulation compared to the peak of the primary shedding in the power spectrum for the sphere wake flow is higher than the peak for the cylinder wake and is shifted to a higher Strouhal-number of $Sr = 0.05$. The primary peak at $Sr = 0.187$ for the sphere wake falls well within the range of values reported by Sakamoto & Haniu⁶ and Tomboulides et al.⁷. Besides these comments, the results revealed much more interesting features which will be published elsewhere due to the limited space herein.

Figure 8 gives an example of the transition of the sphere wake with increasing Reynolds-numbers. For $Re = 280$ the wake is continuous and consists clearly of a pair of attached streamwise vortices. A slight waviness in the size and strength of the vortices can be seen. For $Re = 400$, hairpin-vortices are periodically shed in the wake as described above. Finally, in the case when $Re = 700$ the wake structure allows us to recognize phases, in which - besides an irregular orientation of the hairpin-vortices - the shedding is partly suppressed and the structure is twisted as a whole to a double-helical vortex structure. Such a phase is shown in Fig. 8 at the right-hand side. One can see the beginning and end of this phase by means of the open legs at the top and bottom end of the structure, which mark the generation of the shed hairpin with opposite circulation.

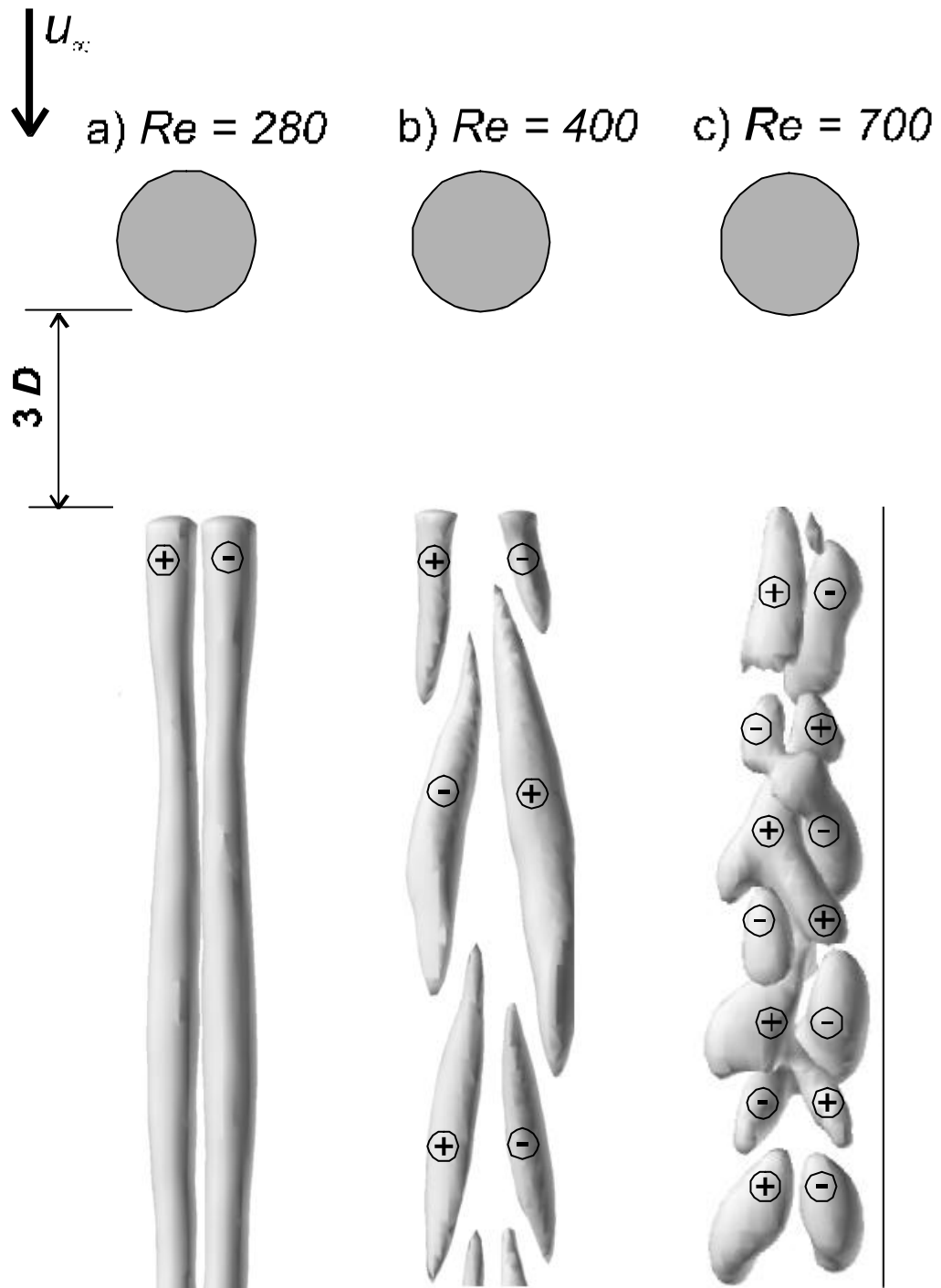


Fig. 8: Spatio-temporal reconstruction of streamwise vorticity distribution in the wake of a sphere for three different Reynolds-numbers.

CONCLUSION

The instability of the wake of an axi-symmetric bluff body originates from the absolute instability against helical waves as demonstrated by Monkewitz⁸ for a family of general axisymmetric wake profiles. With a global stability analysis of the steady sphere wake, Natarajan & Acrivos⁹ could show, that the first instability appears for a non-fluctuating helical wave with an azimuthal wave-number of $k = 1$ (this means that the wave-length fits once within the circumference), i.e. the wake becomes asymmetric but remains steady. Beyond this first critical Reynolds-number, the flow becomes unstable against fluctuating helical waves with $k = 1$, and the flow becomes unsteady. In a numerical study using DNS and a Fourier-description in the azimuthal direction, Schwarz et al.¹⁰ studied the wake of a streamwise oriented cylindrical rod with an elliptic nose and a plane base with a sharp trailing edge. In particular, they studied the amplification and spectra for different modes of helical waves. They proved that the dominant amplified waves in the wake of the simplified bluff body are helical waves with an azimuthal wave-number of $k = 1$. At a Reynolds-numbers of $Re = 400$ the wake was steady and axisymmetric for the chosen geometry. By imposing a small initial disturbance, they could prove for $Re = 500$ the amplification of two counter-rotating helical waves. These long waves were of very low frequency and had a Strouhal-number of $Sr = 0.015$, and were observed to result in the flow pattern as two streamwise vortex filaments. After nonlinear saturation the counter-rotating waves reached the same amplitude and phase velocity which yielded a perfect planar oscillations of the wake (this can be proved by simple additive superposition of both waves). For a higher Reynolds-number when $Re = 700$, the helical waves were further amplified and additional modes were generated by nonlinear interaction, leading to an intermittent discharge of vortex loops at a Strouhal-number of $Sr = 0.133$. In between the periods with regular shedding, phases of domination of one of the helical waves were observed, in which the orientation of the loops changed or the shedding was completely suppressed and the wake was twisted. With the measurement technique described here, we could prove for the first time the observations of Schwarz et al. from quantitative experimental data and confirmed that the wake instability results in similar flow pattern for different axi-symmetric objects. However, the boundary layer thickness influences the critical Reynolds-number at which the wake transforms. Our results let recognize, that a larger boundary thickness shifts the critical Reynolds-number to higher values.

LITERATURE

- ¹ I. Nakamura, "Steady wake behind a sphere," *Phys. of Fluids* 19(1), 5-8 (1976).
- ² E. Achenbach, "Vortex shedding from spheres," *J. Fluid Mech.* 62, 209-221 (1974).
- ³ P. Hirsch, "Über die Bewegung von Kugeln in ruhenden Flüssigkeiten," *Z. Angew. Math. Mechan.* 3, 93 (1923).
- ⁴ W. Willmarth, N.E. Hawk and R.L. Harvey, "Steady and unsteady motions and wakes of freely falling disks", *Phys. of Fluids* 7, 197-208 (1964).
- ⁵ T.A. Johnson and V.C Patel, "Flow past a sphere up to a Reynolds Number of 300," *J. Fluid Mech.* 378, 19 – 70 (1999).
- ⁶ H. Sakamoto and H. Haniu, "The formation mechanism and shedding frequency of vortices from a sphere in uniform shear flow," *JFM* 287, 151-171 (1995).
- ⁷ A. Tomboulides, S. A. Orszag and G. E. Karniadakis "Direct and large-eddy simulations of axisymmetric wakes," AIAA paper no. 93-0546 (1993).
- ⁸ A. P. Monkewitz, "A note on the vortex shedding from axisymmetric bluff bodies," *J. Fluid Mech.* 192, 561. (1988).
- ⁹ R. Natarajan and A. Acrivos, "The instability of the steady flow past spheres and disks," *J. Fluid Mech.* 254, 323-344 (1993)
- ¹⁰ V. Schwarz, H. Bestek and H. Fasel, "Numerical simulation of nonlinear waves in the wake of an axisymmetric bluff body," AIAA paper no. 94-2285 (1994).